The impact of electrodic adsorption on Zn, Cd and Pb speciation measurements with AGNES

J. Galceran*, M. Lao, C. David, E. Companys, C. Rey-Castro, J. Salvador and J. Puy.

Departament de Química and AGROTECNIO. Universitat de Lleida, Rovira Roure 191, 25198 Lleida, Spain

* corresponding author: galceran@quimica.udl.cat

ABSTRACT

The systems assayed in this work (Cd with iodide, Cd with polyacrylic acid, Pb or Zn with xylenol orange, etc.) as well as others previously studied in our lab (Pb/Cd/Zn with humic acids, Pb with pyridinedicarboxylic acid, Pb with organic extracts from river waters, etc.), exhibit induced adsorption of the metallic electroactive species on the mercury electrode. This fact, however, does not hinder the possibility of a correct determination of the free metal concentration in the solution with AGNES (*Absence of Gradients and Nernstian Equilibrium Stripping*). The equilibrium state (the target situation aimed at the end of the deposition stage of AGNES) is not disturbed by induced adsorption, while different strategies (e.g. the use of charge as stripping analytical signal) can avoid a possible kinetic interference on the quantification stage. The impact of adsorption on the blanks proves to be very small and, if needed, it could be further minimized by choosing a sufficiently high gain or variants of AGNES (such as AGNELSV or AGNES-SCP) that do not require the explicit subtraction of the blank. Some surfactants in solution, even without complexing the metal, might block the electrode surface, so that refined methodologies have to be used in such systems. In the case of the dispersant accompanying Nanotek ZnO nanoparticles, the complete blocking of the electrode can be reached in around 100 s, and, thus, electrodes with renovating drops are key for dealing with such kind of difficulties. The free Zn concentration in

equilibrium with these nanoparticles determined by AGNES (with minimization of the deposition times and suppression of any stirring) is consistent with the one expected according to its primary particle size.

Keywords: speciation, nanoparticle, adsorption, AGNES

1. Introduction

The determination of free metal concentrations is important to understand the availability and mobility of toxic metals and micronutrients in environmental and biological systems. Interpretative frameworks such as the Free Ion Activity Model [1] and the Biotic Ligand Model [2,3] point to the free ion concentration as the key variable for the assessment of such availability. Moreover, the modelling of the biogeochemical cycles of metals requires information about the binding properties of ligands, such as natural organic matter, towards these elements, whose experimental determination often requires the specific measurement of the fraction of metal remaining as free ionic species.

The electroanalytical technique AGNES (*Absence of Gradients and Nernstian Equilibrium Stripping*) has been specifically designed to measure free metal ion concentrations [4]. AGNES is a stripping technique consisting of two stages: i) deposition up to an equilibrium situation and ii) quantification of the metal accumulated in the amalgam. Initially, the current under diffusion limited conditions was taken as the response function in the stripping stage (AGNES-I). Up to now, 3 other variants of AGNES are based on the measurement of the charge: AGNES-Q, AGNELSV and AGNES-SCP. AGNES-Q uses the stripped charge along the application of a constant re-

oxidation potential (not necessarily under diffusion limited conditions) [5,6]. In AGNELSV (Absence of Gradients and Nernstian Equilibrium with Linear Stripping Voltammetry) the stripping current is recorded while the potential is scanned at a constant rate [5]. In AGNES-SCP (AGNES with Stripping Chronopotentiomety as second stage), a fixed stripping current is imposed and the evolving potential is recorded [6]. The list of symbols and acronyms can be found as Supporting Information.

AGNES has been applied to the determination of free metal concentrations in a wide range of systems, such as synthetic ligand solutions [6-15], natural samples (sea water[16], river water [17,18] and soil extracts [18]), wine [19,20], solutions containing dissolved organic matter [21-23], clay minerals [24] and also, recently, systems containing quantum dots [25] and ZnO nanoparticles [26-29]. Nevertheless, a rigorous analysis of the relevance of the possible effects of adsorptive processes on the electrode surface regarding the accuracy of AGNES is still lacking. Although induced electrodic adsorption (i.e. adsorption of an electroactive species via formation of a complex) is at the heart of a few electroanalytical techniques (e.g. Cathodic Stripping Voltammetry [30] or AdSCP [31,32]), overcoming its interfering impact has been a challenge for most voltammetric techniques (including Anodic Stripping Voltammetry) [33-35]. The adsorption interference could even jeopardise the validity of large amounts of reported stability constants [36]. Reverse Pulse Polarography (RPP) was shown to be not affected by induced adsorption, but RPP could still be affected by ligand adsorption [37-40]. The minimisation of induced adsorption effects in SCP and SSCP has also been described [41-43].

Adsorption of non-electroactive species can also impact on voltammetric techniques. The fouling of the electrode (resulting from this kind of adsorption) precludes the proper

application of several voltammetric techniques [44,45], being one of the most serious sources of hindrance to reliable measurements of trace metal speciation. Strategies developed for overcoming interferences of adsorption based on the introduction of some modifications of the electrode surface have the inconvenience of their lack of reproducibility [41].

Due to the relative long deposition times in AGNES (typically of the order of 200 to 400 s, but also, of the order of 1000 s or longer, depending on the system and the preconcentration gain), the extent of the various kinds of adsorption might be relevant and, therefore, its possible interference on AGNES measurements should be assessed.

The aim of this work is to study how electrodic adsorption can affect AGNES measurements. The outline of the results follows the possible impact of adsorption on the goals of the first and second stage of AGNES. For the latter, we devote separate sections to those variants of AGNES using current or charge in the quantification step. For this work, a few experimental systems have been selected (iodide, xylenol orange, polyacrylic acid and ZnO nanoparticles) as representatives of different chemical compositions (organic, inorganic) and molecular sizes (monoatomic ions, simple molecules, polymers and particles). These substances have a demonstrated tendency to adsorb on the mercury electrode and, therefore, they constitute suitable benchmarks for the testing of hypothetical interferences on the measurement of Zn, Cd and Pb (the most typical ions probed in voltammetry and having just one oxidation state in solution) with AGNES.

2. Experimental

2.1 Apparatus

The voltammetric measurements were carried out using a μ-AUTOLAB type III potentiostat attached to a Metrohm 663 VA Stand and to a computer by means of the GPES 4.9 (Eco Chemie) and NOVA 1.8 (Eco Chemie) package software. The working electrode was a Metrohm Hanging Mercury Drop Electrode (HMDE) where the smallest drop (drop 1, which according to the catalogue corresponds to a radius $r_0 = 1.41\times10^{-4}$m) was chosen to perform AGNES experiments and the largest drop (drop 3 which corresponds to a radius $r_0=2.03\times10^{-4}$m) to perform Differential Pulse Polarograms (DPP) and Normal Pulse Polarograms (NPP). The auxiliary electrode was a glassy carbon electrode and the reference electrode was Ag|AgCl (3 mol L^{-1}) KCl, encased in a 0.1 mol L^{-1} KNO_3 jacket. Metrohm Ion Selective Electrodes (ISE) for Cd and Pb were used to measure free metal concentration. A CRISON 5203 glass combined electrode was attached to an Orion Research 720A+ ion analyser and introduced in the cell to control the pH. A glass jacketed cell, thermostated at 25.0ºC, was used in all experiments.

2.2 Reagents

Zn, Cd and Pb solutions were prepared from Merck 1000 mg/L standard solutions. Potassium nitrate or potassium chloride was used as supporting electrolytes and prepared from solid KNO_3 and KCl reagents (Fluka, Trace Select), respectively. Xylenol Orange (XO) and potassium iodide solutions were prepared from solid Sigma-Aldrich and Fluka (p.a.), respectively. Tris(hydroxymethyl)aminomethane (Merck, p.a.) and 2-(N-morpholino)ethanesulfonic acid (MES hydrate), (Sigma-Aldrich, >99.5%) were used to prepare buffer solutions to adjust the pH.

Polyacrylic acid, PAA, (Adrich, 35% wt. in water) has an average molecular weight of 250000. Stock solutions of 0.1 M (on a monomer basis) were prepared by dilution

Nanotek ZnO nanoparticles (NP), with a nominal average primary particle diameter of 36 nm (according to the provider), were purchased from AlfaAesar (40% dispersion in water). The characterization data are detailed elsewhere [28]. These ZnO NPs have a surfactant coating in order to stabilize the dispersion, so no sonication was required during sample pretreatment. The exact composition of this additive was not disclosed by the supplier, although ATR-FTIR indicates the coating to be an aliphatic polyether [28]. Despite its stability, Dynamic Light Scattering (using a Malvern Zetasizer Nano ZS) indicates that these NPs are somewhat aggregated in solution, with an average size of 180±8 nm. The analyzed dispersions were prepared by a large dilution of the commercial stock solution to reach an approximate concentration of 2×10^{-4}M in ZnO at pH=8.25 buffered with Tris 0.01M.

In all experiments, ultrapure water (Milli-Q, Millipore) was used.

2.3 Procedures

2.3.1 AGNES

The aim of the first stage or deposition stage of AGNES is to reach a situation of no concentration gradients in the concentration profiles and Nernstian equilibrium, for short *agne* [12]. The absence of gradients implies that, when *agne* is reached, the concentration of free metal at the electrode surface equals to the bulk free metal concentration, both represented by $[M^{2+}]$, while $[M^o]$ stands for the concentration of reduced metal anywhere in the amalgam. Nernst equation can be written as

$$Y = \frac{[M^0]}{[M^{2+}]} = \exp\left[-\frac{2F}{RT}\left(E_1 - E^{0'}\right)\right] \quad (1)$$

where F is the Faraday constant, R the gas constant, T the temperature, E_1 is the applied deposition potential and $E^{o'}$ the formal potential of the redox couple. Y is the gain in metal concentration across the surface due to its preconcentration in the amalgam following the application of E_1 and, in practise, is usually computed from the peak potential of an ancillary DPP experiment with just metal and the background electrolyte [4].

The simplest way (called "1 pulse" or "1P") to achieve the goal of AGNES conditions (*agne*) is to apply the deposition potential (E_1) corresponding to the desired gain (Y) for a sufficiently long time. t_1 designates the period along which E_1 is applied, most of the time with stirring except the last t_w seconds (designated as "waiting time").

Alternatively, in order to reduce the deposition time, the "2 pulses" or "2P" strategy [46] can be implemented, where for $t_{1,a}$ seconds the applied potential $E_{1,a}$ corresponds to diffusion limited conditions for reduction (first substage) and, then, for $t_{1,b}$ seconds the applied potential $E_{1,b}$ corresponds to the desired gain (denoted $Y_{1,b}$, Y_1 or just Y). During the time $t_{1,b}$ (second substage), the desired gain $Y_{1,b}$ is applied in order to compensate any excess (overshoot) or defect (undershoot) of material accumulated along in the first substage until *agne* is reached with the desired gain. Then, a waiting period of duration t_w is also applied at the $Y_{1,b}$ without stirring.

The aim of the second stage is the determination of the concentration of M^0 in the amalgam. The current or the charge in the stripping stage can be measured for this quantification.

2.3.2 Other voltammetric techniques

NPP [47,48] has served to reveal induced adsorption through a peak in the polarogram on top of the usual wave. Used parameters: pulse time 0.05s, interval time 1s, step potential 0.00105 and 0.00495V and base potential -0.4V.

DPP (pages 286-293 in [47]) has been used to establish the desired gains in AGNES. Parameters used: pulse time 0.05s, interval time 1s, step potential 0.00105V and modulation potential 0.04995V.

3. Results and discussion

3.1 Adsorption impact on the first stage

Let us first consider the situation *agne*, reached by the end of the first stage of AGNES (see Section 2.3.1), which includes Nernstian equilibrium between the two forms of the metal (i.e. a fixed relationship between the activities of the amalgamated M^o and M^{2+} in the solution prescribed by the applied potential). In these conditions, fundamental thermodynamic considerations lead to the straightforward conclusion that the presence of an *equilibrated* intermediate phase (such as adsorbed metal, ligand or complex) would not influence the activities of the element related by the Nernstian equation, because the interfacial species would also be in equilibrium with the bulk species. Of course, we are also assuming that the masses of this intermediate phase and the one accumulated in the amalgam are negligible in comparison with the total mass of the analyte in the solution and that the transference of metal between phases is possible.

On the other hand, adsorption could modify the required time for equilibration or even delay it beyond its practical reach. Notice that, for *agne,* it is implicitly required that the amount of adsorbed complex ML (or L or any other connected to M) also fulfils its equilibrium with the bulk concentration of ML [49]. Therefore, any possible impact of

electrodic adsorption on the first stage could only come from kinetic limitations, which can, in principle, be overcome (by waiting until stabilization) except in very dramatic situations (such as perfect blocking of the charge transfer at the electrode surface, see section 3.1.2.)

3.1.1 Induced adsorption

We first consider with more detail the case of induced adsorption where the analyte (the metal M^{2+}) accumulates on the electrode surface, during the deposition stage, via the formation of a complex ML[33].

As illustrative cases, we have probed here a few model systems like Pb+XO [32,50], Zn+XO [51], Cd+PAA [52] and Cd+I [53-55] which have been previously studied in the literature and reported to show induced adsorption on the mercury electrode.

A diagnostic of induced adsorption can be gained from the observation of a peaked NPP. In the particular case of PbXO, the peak is also shifted with respect to the half wave potential (see Fig 1) as predicted for very strong induced adsorption[56]. We have checked that similar phenomena take place with ZnXO (see fig SI-1).

3.1.1.1 Impact of induced adsorption on equilibrium

For the system Cd+PAA, as seen in Fig 2, the values retrieved following the standard application of AGNES are in excellent agreement with the ones obtained by Cd-ISE at the various essayed pH. Notice that other voltammetric techniques require elaborate procedures to retrieve the free Cd concentrations in a system (Cd + polymethacrylic acid) very similar to this one [34,57,58].

Another example of the negligible impact of induced electrodic adsorption on AGNES is given by the Cd-I system (see Fig SI-2). Indeed, AGNES measurements of free Cd^{2+}

concentrations throughout titration experiments with iodide show a good agreement with speciation calculations using literature values (NIST 46.7) of the stability constants for CdI, as shown in Fig 3. In this case, as the ionic strength increases with the addition of relevant amounts of iodide (as also happened in [20]), there is a change in the prescribed gain even if the applied deposition potential is kept constant. This real gain can be computed with eqn (12) of ref. [13], which simplifies to:

$$Y = \frac{\gamma_{M^{2+}}}{\gamma_{M^{2+}}^{\mu=0.1}} Y^{\mu=0.1} \qquad (2)$$

A titration of Pb with XO (see Fig 4) suggests a close agreement between AGNES, and ISE measurements, while the theoretical expectations from literature values of the stability constants [59] are only slightly below the experimental data (note the linear scale in the y-axis, in contrast with other logarithmic scales, e.g., in Fig 2). For additions of XO around 2 μM, the discrepancy between theoretical and experimental results might stem from small inaccuracies in the values of the constants or in the experimental setup.

From these experiments and others performed in our lab with other systems exhibiting induced adsorption (humic acids [21-23], pyridinedicarboxylic acid [7,8], etc.), we conclude that induced adsorption does not distort the final equilibrium of AGNES in any of the systems studied so far, which is consistent with our current physicochemical interpretative framework of equilibrium not being affected by other concomitant side equilibria.

3.1.1.2 Impact of induced adsorption on the kinetics of equilibration

Despite eventually reaching the prescribed *agne*, induced adsorption might delay the practical approach to the equilibrium by blocking the surface or by requiring the slow

transport of a huge amount of ML in order to satisfy its adsorption equilibrium at the electrode surface (i.e. for some strongly adsorbing systems[49]).

In all cases analyzed in our work, we do not have evidence for any case of induced adsorption increasing the deposition times. From a practical point of view, we can set an upper limit to the deposition time as the one needed when only metal is present in the solution. If the required deposition time (for a given gain) in the system with induced adsorption is larger than the only-metal deposition time, we would know that the kinetic impact of adsorption has been large enough to overcompensate the contribution of the complexes to the flux (which shortens the deposition times unless they are totally inert complexes). The required deposition times depend on the program used for the first stage: either 1P (the simplest one) or 2P [46]. In our experience [12], for HMDE the rules for a sufficiently long deposition time are:

$$\begin{aligned} t_1 - t_w &= 7\,Y \qquad 1-\text{Pulse} \\ t_{1,a} &= 0.7\,Y \qquad 2-\text{Pulses} \end{aligned} \tag{3}$$

Fig 5 indicates that t_1-t_w≈200 s is enough to reach a gain of 50 and t_1-t_w≈500 s is enough for Y=200, which are much shorter than the times derived from the rule (350 s and 2800 s, respectively). This also means that the contribution of the complexes (possibly very labile) shortens the deposition time more than the increase in deposition time (if any) due to adsorption.

For PbXO under other conditions (of concentrations and pH), as well as for the other systems studied in this work, the comparison has always indicated that the possible delay of the adsorption on the deposition time is shorter than the reduction of time arising from the contribution of the complexes, so that the standard rules (3) continue to be useful guidelines.

3.1.2 Blockage of the electrode by surfactants

On the other hand, AGNES equilibrium could not be reached in a reasonable deposition time when there is some compound that quickly adsorbs onto the electrode surface to form a film, so densely packed and so strongly bound, as to kinetically hinder the reduction and oxidation processes.

We have found this blocking behaviour (or fouling, [44]) when studying the dissolution equilibrium of Nanotek ZnO nanoparticles, as a follow up of our work with other nanoparticles [26]. The particularity of these NPs (in comparison to other NPs in our previous work) is the presence of an aliphatic polyether coating [28], which acts as a dispersant to stabilize the ZnO suspensions, and whose exact composition is not disclosed by the manufacturer.

The undistorted shape of the NPP (see Fig SI-3) of the dispersion of NPs at pH=8.25 does not reveal induced adsorption. The DPP (Fig SI-4) in a solution containing the dispersant (e.g. a sample of Nanotek NPs at a sufficiently low pH, where all the ZnO is dissolved) is practically identical to polarograms of Zn^{2+} solutions in absence of the dispersant. Moreover, the lack of shift from pH=8.2 to pH=4.0 in the DPP peak measured in Nanotek samples (see SI-4) also indicates that the dispersant does not extensively complex Zn, so -if there is any induced adsorption-, it would have a negligible impact on AGNES. Furthermore, the lack of distortions also suggest that dispersant adsorption during the short time of pulse polarography (1 s) without stirring is mild.

Despite these findings, the performance of AGNES reveals some kind of interference due to the presence of the dispersant. Fig 6 shows a plot of a strategy typically used in previous works to adjust the deposition times $t_{1,a}$ and $t_{1,b}$ [19,23]. For non-complicated systems, one usually finds that too long $t_{1,a}$-values produce overshoots (i.e. values above

the equilibrium) which progressively decay to the equilibrium value for increasing times $t_{1,b}$, while for short $t_{1,a}$-values the undershoot has to be compensated with additional (longer) $t_{1,b}$ times; but in all cases there is a convergence towards the equilibrium concentration. In Fig 6, however, we find that the different series (for different $t_{1,a}$) do not completely converge to any common equilibrium value for the huge $t_{1,b}$ time of 3000 s. Indeed, we would expect [46] that within $t_{1,b}$=3 $t_{1,a}$, which is less than 25 s for all the series, *agne* was reached at the longest $t_{1,b}$-values shown in this figure. So, we conclude that there is some kind of blockage of the electrode surface or other irreversibilities affecting the redox process (notice that the blocking can also be considered an irreversibility, see p 623 in [47]). We discuss first the hypothesis of the surfactant blocking the electrode surface.

In order to see how the blockage proceeds with time, we repeated dedicated experiments without dislodging the drop in between them. Thus, each of the 3 series in Fig 7 corresponds to successive experiments performed with one drop immersed in a dispersion of Nanotek NPs. In experiments with blue circle markers, Zn was accumulated at Y=10 for a time t_1=10s (with stirring and without any waiting period, t_w=0). We caution that these are not AGNES experiments (but rather ancillary ones) because we do not check that *agne* is reached. The retrieved currents decrease steeply after the first 25 seconds down to a practically negligible value, consistent with the hypothesis of the blocking dispersant being adsorbed in a very short time due to the facilitation of mass transport with the stirring. The repetition of the same potential program with another drop (see green square markers), but without stirring (same total deposition time, i.e.: t_1=t_w=10s), shows that the period before total blocking without stirring is longer than that with stirring. This can be understood as due to a transport limitation of the dispersant needed for total blocking of the electrode surface. We conclude that, for this system where

304 blocking is diffusion limited (while the required gains are small), it is convenient to avoid
305 stirring in the deposition stage of AGNES. We also see that, without stirring, there are
306 around 100 s left before total blocking is attained (for this gain), so, in the final design of
307 the parameters we seek to have total deposition times shorter than 100 s. Red triangle
308 markers in Fig 7 correspond to a very negative deposition potential: we see that, despite
309 the time elapsed (since the formation of the drop) and the amount of adsorbed dispersant,
310 no change in the current appears within the drop lifetime, indicating that Zn^{2+} converts
311 into Zn^{o} at $Y=10^{12}$ and, also, that Zn^{o} converts into Zn^{2+} at $Y=10^{-10}$.

312 In order to elucidate whether the application of a very negative potential ($Y=10^{12}$) might
313 clean the electrode surface from surfactants [35], we alternated in just one series (i.e. in
314 just one drop) the previous two series without stirring (now, subseries). As seen in Fig 8,
315 after 200 s of drop lifetime, the first subseries at $Y=10$ indicates full blockage. The
316 application of the second subseries, at $Y=10^{12}$ is not affected by this full blockage. The
317 third subseries, again at $Y=10$, indicates that reduction of Zn^{2+} is hindered to the same
318 extent as at the end of the first subseries, so that the very negative potential (applied in
319 the previous subseries from 200 to 400 s of drop life) does not seem to remove the
320 surfactant away from the electrode surface. The progress of the blockage with time is also
321 clearly confirmed by cyclic voltammetry (see Fig SI-5).

322 From a practical point of view, we conclude that AGNES has to be applied without
323 stirring along a deposition time that should be as short as possible (below 100 s for our
324 conditions), reach *agne* and proceed to the stripping stage and, then, start with a new drop
325 for the next experiment. Renovating mercury electrodes (such as HMDE) are, in this
326 respect, more convenient than Rotating Disk Electrodes, Screen Printed Electrodes or
327 microelectrodes, given that with a fixed mercury film one could not avoid or reverse the

328 blocking of the surface (see page 569 in [47]). AGNES 2P can cut the deposition time
329 down to a minimum with a suitable $t_{1,a,w}$ (where subscript w recalls that no stirring is
330 applied) to accumulate in the drop almost the exact amount of Zn^o needed for *agne* at the
331 prescribed gain in the solution of interest.

332 In order to find a deposition time close to the optimum $t_{1,a,w}$ value, we designed a new
333 kind of ancillary experiments (in this case, each series corresponds to a new drop). We
334 call Exp1 to experiments where we allow for a short second substage of the deposition
335 program (i.e. $t_{1,b}$=0; $t_w \neq 0$) to approach equilibrium at the desired gain. We call Exp2 to
336 experiments where the stripping stage immediately follows the diffusion limited
337 deposition substage ($t_{1,b}=t_w=0$), so that we assess the amount of material that has entered
338 along the first substage. For $t_{1,a,w}$ shorter than the optimum one (undershoot), the substage
339 at the desired gain will accumulate more Zn^o in the drop, so that I(Exp1)>I(Exp2).
340 Conversely, for $t_{1,a,w}$ longer than the optimum one (overshoot), I(Exp1)<I(Exp2) because
341 the fine-tuning substage of Exp1 tends to remove Zn^o from the amalgam. In the particular
342 case of Fig 9, we aim at a gain of Y=5 (given that the free Zn concentration in this NP
343 dispersion is quite high). The intersection of the series of Exp1 and Exp2 should provide,
344 in principle, an optimum $t_{1,a,w}$ around 10s (which is sufficiently away from the total
345 blockage time of 100 s). In practice, with just $t_{1,a,w}$=10s, an undershoot was very clear.
346 The application of $t_{1,a,w}$= 12.5 and 15 s with t_w=10, 50, 100 and 200 s provides
347 concentrations listed in Table 1. The application of the same methodology with different
348 gains leads to approximately a proportionally longer or shorter optimum $t_{1,a,w}$, but
349 essentially the same free metal concentration.

Fig 10 shows that the average [Zn^{2+}] experimental value of 1.04×10^{-5}M falls within the range of theoretically expected concentrations for diameters in between 36±15 nm at this pH-value, when applying eqn. 5 from ref. [26]:

$$\left[Zn^{2+}\right]_{NP} = \left[Zn^{2+}\right]_{bulk} \exp\left\{\frac{3.76}{r_{NP}/\mathrm{nm}}\right\} \quad (4)$$

where $\left[Zn^{2+}\right]_{NP}$ and $\left[Zn^{2+}\right]_{bulk}$ indicate the concentrations of free Zn in equilibrium with the studied NP and with the bulk material, respectively. Non-blocking irreversibilities [60,61], associated to a sluggish kinetics of the electron transfer, could delay the reaching of *agne.* If this case appeared, checking the attainment of a constant response function in the second stage with increasing deposition times would overcome the difficulty (see section 3.1.1.2). Moreover, simple calculations (not shown), parallel to those in ref. [62], suggest that, using parameters typical of Zn electrodic processes without specific adsorption [63,64], the electron transfer is not the limiting stage by the end of the relatively long deposition stage. Experimentally, we have not found yet any impact of (a possible) irreversibility in none of the Zn systems explored here, nor with oxalate[6,46], seawater[16], humic acids [21], or river water[17,18]. In the case of Zn in wine[19], we speculated that irreversibility might be responsible for the anomalously long $t_{1,b}$ required, and this irreversibility could perhaps be also due to a partial blockage. In the present case of Nanotek nanoparticles, we cannot rule out some irreversibility not related to the blockage, but the good results for a sufficiently short (optimized) $t_{1,a,w}$-value clearly suggest that the existing difficulties have been overcome.

3.2 Adsorption impact on the AGNES stripping diffusion limited current

Most of the work done with AGNES has used the intensity current under diffusion limited conditions (read at a fixed stripping time t_2) as a way of fulfilling the quantification mission of the second stage (AGNES-I). The faradaic current I_f can be

obtained from the measured current by subtraction of a blank (mostly capacitive current), such as the synthetic blank, with just background electrolyte [4]. The value t_2=200 ms has been selected because most of the capacitive current is expected to be extinguished at that time (see section 1.2.4 in ref. [47]), so that the ratio noise/signal is minimum [4].

Because of the linear nature of the diffusion equation inside the drop, it can be shown that, regardless of the geometry of the electrode, in the AGNES-I variant, the faradaic current is proportional to the free metal ion concentration [4]:

$$I_f = Y\eta\left[M^{2+}\right] \quad (5)$$

The normalized proportionality factor η can be found from a calibration.

The faradaic current under diffusion limited conditions cannot be affected by any phenomenon in the solution [4,37], so that, in principle, I_f is independent of electrodic adsorption. These conditions do not apply when intermetallic compounds are formed[12], when the solubility of Zn^o, Pb^o or Cd^o in Hg is approached [5] or when the metal in solution has more than one oxidation state (which is not the case for the 3 metals studied in this work).

However, adsorption might impact AGNES determination via the blank, given that adsorption can modify the capacitive current (i.e. by changing the double layer structure)[65]. For instance, the synthetic blank (where only the background electrolyte is present in the medium) might be not fully representative of the capacitive current when L or ML are adsorbed onto the electrode surface at a very different extent between the deposition and stripping potentials. Similar considerations to those justifying the use of the synthetic blank when charge is the analytical signal (see next section) also apply here to the current.

3.3 Adsorption impact on the stripped faradaic charge

Alternatively to the current, a response function to quantify the amount of accumulated Mº is the total stripped faradaic charge, Q_f. The combination of Nernst and Faraday laws allows writing [5,15]:

$$Q_f = nFV_{Hg}[M^o] = \eta_Q Y[M^{2+}] \quad (6)$$

η_Q is the normalized proportionality factor (usually obtained by calibration) and should only depend on the volume of mercury.

As mentioned in Section 1, up to now, 3 variants of AGNES have exploited Q_f: AGNES-Q, AGNELSV and AGNES-SCP.

Induced adsorption could impact on the evolution of the transient stripping current in AGNES-Q or AGNELSV or the recorded potential in AGNES-SCP, but not on the eventual value of the total faradaic charge associated to the amount of Mº accumulated at equilibrium. In the second stage, we re-oxidate Mº, so the presence of adsorbed ML is irrelevant for the stripped charge Q_f (because ML –either adsorbed or in solution- cannot be neither oxidized nor reduced at the stripping potential E_2).

Only the variant AGNES-Q requires a blank. The synthetic blank yields the charge of the same potential program with just background electrolyte. The change in the double layer structure due to adsorption might impact on the blank, as in AGNES-I (but to a lesser extent if the potential jump is smaller because E_2 does not correspond to diffusion limited conditions). The treatment detailed in the Supporting Information indicates that, for the assayed systems, the charge of the blank is a reasonable surrogate for the capacitive charge. Furthermore, as with AGNES-I, the selection of a sufficiently high gain Y usually renders the specific value of the blank negligible. Thus, the total charge (summation of

faradaic and capacitive charge) is practically constant for all stripping potentials (E_2) because the changes in $Q_{cap}(\infty)$ (due to the variation in E_2-E_1) are negligible in front of Q_f (see, for instance, Fig SI-6).

Free concentrations determined with AGNES-Q are comparable with those of AGNES-I, see, for instance, Figs 3 and 4, confirming also the low impact of induced adsorption on the computed Q_f.

In AGNELSV the stripping current is recorded while the potential is scanned at a sufficiently slow constant rate from the deposition potential E_1 up to a sufficiently less negative potential so that all Mº has been reoxidated[5] (see Fig SI-7 for a schematic representation of the potential program). In principle, in AGNELSV there is no need to subtract a blank, given that Q_f can be computed from the area above the baseline (which is assumed to contain the capacitive current). Indeed, the baseline of a system with constant capacity C (in the range of linearly swept potentials $E=E_1+vt$) is a horizontal straight line in the plot I vs E:

$$I_{cap} = \frac{d[C\,E]}{dt} = \frac{d[C\,(E_1 + v\,t)]}{dt} = C\,v \qquad (7)$$

This line should merge with the horizontal section of the experimental curve (when the faradaic processes are absent). However, adsorption might produce a non-constant C. Assuming a linear dependency of the capacitance with the potential:

$$C = C_1 + \frac{(C_2 - C_1)}{(E_2 - E_1)}(E - E_1) = C_1 + \frac{(C_2 - C_1)}{(E_2 - E_1)}vt \qquad (8)$$

one finds a straight line for the capacitive current in an I vs E plot:

$$I_{cap} = C_1 v + E_1 \frac{(C_2 - C_1)}{(E_2 - E_1)}v + 2\frac{(C_2 - C_1)}{(E_2 - E_1)}v^2 t = C_1 v + E_1 \frac{(C_2 - C_1)}{(E_2 - E_1)}v + 2\frac{(C_2 - C_1)}{(E_2 - E_1)}v(E - E_1) \qquad (9)$$

442 and the computation of Q_f could be done from the area above this straight base line. One
443 way of detecting a varying C would consist in repeating the scan without any Mº
444 preconcentrated (to minimize Q_f), but this is just an ideal situation. We see in Fig 11, that
445 for the case Cd+I, the AGNELSV curve is a practically straight line, so we took the
446 baseline of the various experiments with Cd+I as the prolongation of the straight region at
447 the right of the plot (when the peak associated to the faradaic current is clearly vanished).
448 Examples of retrieved AGNESLV voltammograms are shown in Fig SI-8.

449 The normalized proportionality factor η_Q found from the variant AGNELSV in various
450 calibrations compare very well with other variants (see Table SI-1) and with literature
451 values [15]. Small variations around 0.002 C/M between the different metals can be
452 ascribed to inaccuracies in the determination of the gains (such as inaccurate diffusion
453 coefficients or in the determination of the DPP E_{peak}), but such offsets cancel out between
454 the corresponding calibration and measurement, so that the retrieved free concentrations
455 are reliable.

456 The third variant using the charge as response function is AGNES-SCP. As in
457 AGNELSV, in principle, no blank is needed (see SI of reference [15]), and one just reads
458 the transition time, τ, from the area above the baseline. The η_Q-values found in
459 calibrations are similar to those of other variants (see Table SI-1). The retrieved free
460 concentration values obtained with this variant agree with the results of other variants and
461 with theoretical speciation calculations (see Fig 3). The lack of impact of complex
462 adsorption on the peak area using a SCP program with full depletion has already been
463 shown theoretically and experimentally [41].

464

4. Conclusions

When the principles of AGNES are met (i.e. when the aims of each stage are fulfilled), electrodic adsorption is not expected to preclude the determination of the free metal concentration.

If the special equilibrium situation (*agne*) aimed at by the first stage is reached, the existence of other side equilibria (such as adsorption processes) should not impact on the amount of accumulated M^o (see section 3.1.1). Quantification in the second stage can be performed via the diffusion-limited faradaic intensity current (variant AGNES-I, see section 3.2) or via the total faradaic charge (variants AGNES-Q, AGNELSV and AGNES-SCP, see section 3.3). The diffusion-limited faradaic current cannot be affected by any process in solution (such as adsorption). Electrodic adsorption cannot affect the faradaic charge, either, because this charge is just proportional to the accumulated M^o (see eqn. (6)). Adsorption can impact on the total current or the total charge via changes in the double layer, so that suitable blanks (or a suitable baseline, in the case of AGNES-SCP) have to be subtracted. Fortunately, in practice, by sufficiently increasing the gain Y, one can render this capacitive current or charge negligible in front of the faradaic one, so that accurate concentrations can be finally obtained even if the capacitive estimation (via the blank measurement) is not excellent.

Experimental results in a wide variety of systems where induced electrodic adsorption is apparent confirm that AGNES yields accurate values of the free metal ion concentrations. Apart from systems in previous papers, this has also been shown here in the cases of Cd+Poly(acrylic) acid (fig. 2), Cd+I (Fig.3) and Pb+Xylenol Orange (Fig.4).

The blockage or total fouling of the electrode can be a much more serious problem than induced electrodic adsorption. For instance, see Figs 7 and 8, the dispersant

accompanying Nanotek ZnO NPs seems to block the electrode in a relatively short time. In this case, it is essential to optimize the deposition time and turn the stirring off (see Fig 9) to reach the equilibrium conditions (*agne*) before the total blockage.

Acknowledgements

Experiments with PAA were conducted with the help of Antoni Ortín and Anna Sedó, whose contribution is gratefully acknowledged. The authors gratefully acknowledge support of this research by the Spanish Ministry Spanish Ministry of Education and Science (Projects CTQ2009-07831 and CTM2012-39183), by the "Comissionat d'Universitats i Recerca de la Generalitat de Catalunya" and by the European Union Seventh Framework Programme (FP7-NMP.2012.1.3-3) under grant agreement no. 310584 (NANoREG). R. Wallace, N. Hondow, A.P. Brown, S.J. Milne and R. Brydson (Institute for Materials Research, University of Leeds, UK) are gratefully acknowledged for providing a characterized sample of the Nanotek ZnO nanoparticles (EN-Z-1) with funding from the European Union Seventh Framework Programme FP7-NMP-2008-1.3-2, grant agreement 229244 (ENNSATOX).

5. References

Reference List

[1] A.Tessier, J.Buffle, P.G.C.Campbell, in J. Buffle and R. R. DeVitre (Eds.), Chemical and Biological Regulation of Aquatic Systems, Lewis Publishers, Boca Raton, FL, 1994, Chapter 6, p. 197.

[2] P.G.C.Campbell, O.Errecalde, C.Fortin, W.R.Hiriart-Baer, B.Vigneault, Comp. Biochem. Physiol. C 133 (2002) 189.

[3] P.R.Paquin, J.W.Gorsuch, S.Apte, G.E.Batley, K.C.Bowles, P.G.C.Campbell, C.G.Delos, D.M.Di Toro, R.L.Dwyer, F.Galvez, et al. Comp. Biochem. Physiol. C 133 (2002) 3.

[4] J.Galceran, E.Companys, J.Puy, J.Cecília, J.L.Garcés, J. Electroanal. Chem. 566 (2004) 95.

[5] J.Galceran, D.Chito, N.Martinez-Micaelo, E.Companys, C.David, J.Puy, J. Electroanal. Chem. 638 (2010) 131.

[6] C.Parat, D.Aguilar, L.Authier, M.Potin-Gautier, E.Companys, J.Puy, J.Galceran, Electroanal. 23 (2011) 619.

[7] G.Alberti, R.Biesuz, C.Huidobro, E.Companys, J.Puy, J.Galceran, Anal. Chim. Acta 599 (2007) 41.

[8] C.Huidobro, E.Companys, J.Puy, J.Galceran, J.P.Pinheiro, J. Electroanal. Chem. 606 (2007) 134.

[9] R.F.Domingos, C.Huidobro, E.Companys, J.Galceran, J.Puy, J.P.Pinheiro, J. Electroanal. Chem. 617 (2008) 141.

[10] J.P.Pinheiro, J.Salvador, E.Companys, J.Galceran, J.Puy, Phys. Chem. Chem. Phys. 12 (2010) 1131.

[11] L.S.Rocha, E.Companys, J.Galceran, H.M.Carapuca, J.P.Pinheiro, Talanta 80 (2010) 1881.

[12] D.Chito, J.Galceran, E.Companys, Electroanal. 22 (2010) 2024.

[13] D.Aguilar, C.Parat, J.Galceran, E.Companys, J.Puy, L.Authier, M.Potin-Gautier, J. Electroanal. Chem. 689 (2013) 276.

[14] D.Aguilar, J.Galceran, E.Companys, J.Puy, C.Parat, L.Authier, M.Potin-Gautier, Phys. Chem. Chem. Phys. 15 (2013) 17510.

[15] C.Parat, L.Authier, D.Aguilar, E.Companys, J.Puy, J.Galceran, M.Potin-Gautier, Analyst. 136 (2011) 4337.

[16] J.Galceran, C.Huidobro, E.Companys, G.Alberti, Talanta 71 (2007) 1795.

[17] F.Zavarise, E.Companys, J.Galceran, G.Alberti, A.Profumo, Anal. Bioanal. Chem. 397 (2010) 389.

[18] D.Chito, L.Weng, J.Galceran, E.Companys, J.Puy, W.H.van Riemsdijk, H.P.van Leeuwen, Sci. Total Envir. 421-422 (2012) 238.

[19] E.Companys, M.Naval-Sanchez, N.Martinez-Micaelo, J.Puy, J.Galceran, J. Agric. Food Chem. 56 (2008) 8296.

[20] D.Chito, J.Galceran, E.Companys, J.Puy, J. Agric. Food Chem. 61 (2013) 1051.

[21] E.Companys, J.Puy, J.Galceran, Environ. Chem. 4 (2007) 347.

548 [22] J.Puy, J.Galceran, C.Huidobro, E.Companys, N.Samper, J.L.Garcés, F.Mas,
549 Environ. Sci. Technol. 42 (2008) 9289.

550 [23] B.Pernet-Coudrier, E.Companys, J.Galceran, M.Morey, J.M.Mouchel, J.Puy,
551 N.Ruiz, G.Varrault, Geochim. Cosmochim. Ac. 75 (2011) 4005.

552 [24] E.Rotureau, Colloids Surf. A 441 (2014) 291.

553 [25] R.F.Domingos, D.F.Simon, C.Hauser, K.J.Wilkinson, Environ. Sci. Technol. 45
554 (2011) 7664.

555 [26] C.David, J.Galceran, C.Rey-Castro, J.Puy, E.Companys, J.Salvador, J.Monné,
556 R.Wallace, A.Vakourov, J. Phys. Chem. C 116 (2012) 11758.

557 [27] N.Adam, C.Schmitt, J.Galceran, E.Companys, A.Vakourov, R.Wallace,
558 D.Knapen, R.Blust, Nanotoxicology 8 (2013) 709.

559 [28] Q.Mu, C.A.David, J.Galceran, C.Rey-Castro, L.Krzemiñski, R.Wallace,
560 F.Bamiduro, S.J.Milne, N.S.Hondow, R.Brydson, G.Vizcay-Barrena,
561 M.N.Routledge, L.J.C.Jeuken, A.P.Brown. A systematic investigation of the
562 physico-chemical factors that contribute to the toxicity of ZnO nanoparticles.
563 Accepted. Chemical Research in Toxicology, 2014;

564 [29] R.F.Domingos, Z.Rafiei, C.E.Monteiro, M.A.K.Khan, K.J.Wilkinson, Environ.
565 Chem. 10 (2013) 306.

566 [30] C.M.G.van den Berg, Talanta 31 (1984) 1069.

567 [31] H.P.van Leeuwen, R.M.Town, J. Electroanal. Chem. 610 (2007) 9.

568 [32] R.M.Town, H.P.van Leeuwen, J. Electroanal. Chem. 610 (2007) 17.

569 [33] H.P.van Leeuwen, J.Buffle, M.Lovric, Pure Appl. Chem. 64 (1992) 1015.

570 [34] A.M.Garrigosa, J.M.Diaz-Cruz, C.Arino, M.Esteban, Electrochim. Acta. 53
571 (2008) 5579.

572 [35] Y.Louis, P.Cmuk, D.Omanovic, C.Garnier, V.Lenoble, S.Mounier, I.Pizeta,
573 Anal. Chim. Acta 606 (2008) 37.

574 [36] A.M.Bond, G.Hefter, J. Electroanal. Chem. 68 (1976) 203.

575 [37] J.Galceran, D.Rene, J.Salvador, J.Puy, M.Esteban, F.Mas, J. Electroanal. Chem.
576 375 (1994) 307.

577 [38] J.Puy, M.Torrent, J.Monné, J.Cecília, J.Galceran, J.Salvador, J.L.Garcés, F.Mas,
578 F.Berbel, J. Electroanal. Chem. 457 (1998) 229.

579 [39] E.Companys, J.Puy, M.Torrent, J.Galceran, J.Salvador, J.L.Garcés, F.Mas,
580 Electroanal. 15 (2003) 452.

581 [40] J.P.Pinheiro, A.M.Mota, M.L.S.S.Gonçalves, M.Vanderweijde, H.P.van Leeuwen,
582 J. Electroanal. Chem. 410 (1996) 61.

583 [41] R.M.Town, H.P.van Leeuwen, J. Electroanal. Chem. 523 (2002) 1.

584 [42] R.M.Town, H.P.van Leeuwen, J. Electroanal. Chem. 541 (2003) 51.

585 [43] N.Serrano, J.M.Díaz-Cruz, C.Ariño, M.Esteban, J.Puy, E.Companys, J.Galceran,
586 J.Cecilia, J. Electroanal. Chem. 600 (2007) 275.

587 [44] M.L.Tercier, J.Buffle, Anal. Chem. 68 (1996) 3670.

588 [45] B.Hoyer, N.Jensen, Analyst. 129 (2004) 751.

589 [46] E.Companys, J.Cecília, G.Codina, J.Puy, J.Galceran, J. Electroanal. Chem. 576
590 (2005) 21.

591 [47] A.J.Bard, L.R.Faulkner, Electrochemical Methods. Fundamentals and
592 Applications., Second edition ed. John Wiley & Sons, Inc., New York, 2001.

593 [48] J.Galceran, J.Salvador, J.Puy, J.Cecília, M.Esteban, F.Mas, Anal. Chim. Acta 305
594 (1995) 273.

595 [49] H.P.van Leeuwen, R.M.Town, Environ. Sci. Technol. 39 (2005) 7217.

596 [50] Q.G.Wu, G.E.Batley, Anal. Chim. Acta 309 (1995) 95.

597 [51] A.A.Ensafi, A.Benvidi, T.Khayamian, Analytical letters 37 (2004) 449.

598 [52] J.M.Díaz-Cruz, C.Ariño, M.Esteban, E.Casassas, Electroanal. 3 (1991) 299.

599 [53] M.Zelic, M.Lovric, J. Electroanal. Chem. 541 (2003) 67.

600 [54] E.Guaus, F.Sanz, Electroanal. 11 (1999) 424.

601 [55] E.Casassas, C.Arino, J. Electroanal. Chem. 213 (1986) 235.

602 [56] J.Puy, J.Salvador, J.Galceran, M.Esteban, J.M.Díaz-Cruz, F.Mas, J. Electroanal.
603 Chem. 360 (1993) 1.

604 [57] F.Mas, J.Puy, J.M.Díaz-Cruz, M.Esteban, E.Casassas, Anal. Chim. Acta 273
605 (1993) 297.

606 [58] J.Puy, F.Mas, J.M.Díaz-Cruz, M.Esteban, E.Casassas, Anal. Chim. Acta 268
607 (1992) 261.

608 [59] S.Murakami, K.Ogura, T.Yoshino, Bull. Chem. Soc. Jpn. 53 (1980) 2228.

609 [60] A.M.Mota, M.M.Correia dos Santos, in A. Tessier and D. R. Turner (Eds.), Metal
610 Speciation and Bioavailability in Aquatic Systems, John Wiley & Sons,
611 Chichester, 1995, Chapter 5, p. 205.

612 [61] F.Berbel, J.M.Díaz-Cruz, C.Ariño, M.Esteban, J. Electroanal. Chem. 475 (1999)
613 99.

614 [62] H.P.van Leeuwen, R.M.Town, J. Electroanal. Chem. 556 (2003) 93.

[63] D.Omanovic, M.Branica, J. Electroanal. Chem. 565 (2004) 37.

[64] G.Lopez-Perez, R.Andreu, D.Gonzalez-Arjona, J.J.Calvente, M.Molero, J. Electroanal. Chem. 552 (2003) 247.

[65] M.Lovric, J. Electroanal. Chem. 170 (1984) 143.

6. Table

Table 1:Free Zn concentration obtained from the application of AGNES with the optimized deposition time under diffusion limited conditions without stirring to a dispersion of Nanotek ZnO NPs around 2×10^{-4}M, pH=8.29 , [KCl]=0.1M

$[Zn^{2+}]$ / M	$Y = 2$; $t_{1,a,w} = 3$ s	$Y = 5$; $t_{1,a,w} = 12.5$ s	$Y = 5$; $t_{1,a,w} = 15$ s
$t_w = 10$ s	$(8.69\pm 0.21) \times 10^{-6}$	$(9.65\pm 0.08) \times 10^{-6}$	$(1.08\pm 0.02) \times 10^{-5}$
$t_w = 50$ s	$(1.02\pm 0.01) \times 10^{-5}$	$(1.02\pm 0.02) \times 10^{-5}$	$(1.03\pm 0.01) \times 10^{-5}$
$t_w = 100$ s	$(1.05\pm 0.01) \times 10^{-5}$	$(1.02\pm 0.01) \times 10^{-5}$	$(1.05\pm 0.01) \times 10^{-5}$
$t_w = 200$ s	$(1.04\pm 0.01) \times 10^{-5}$	$(1.02\pm 0.01) \times 10^{-5}$	$(1.05\pm 0.01) \times 10^{-5}$

7. Figures

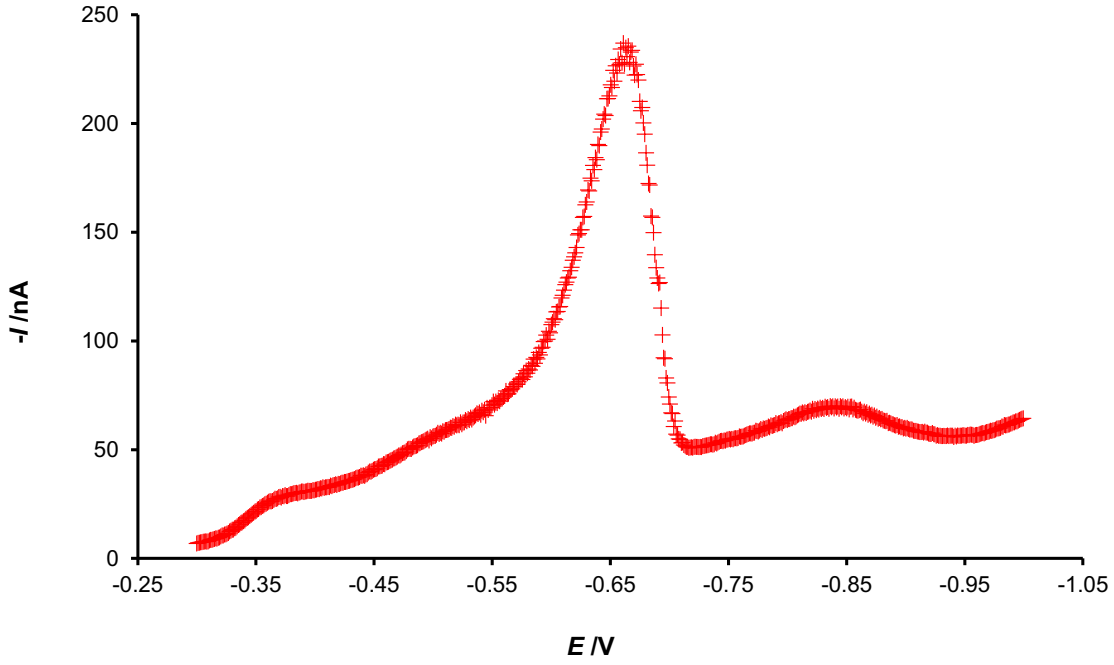

Figure 1: Normal Pulse Polarogram in the system Pb+xylenol orange, showing the typical peak of strong induced adsorption. $c_{T,Pb}$= 1.57 x 10^{-5}M, $c_{T,XO}$= 8.99 x 10^{-6}M and pH= 6.802 in 0.1 M KNO_3. E_{base}= -0.1 V

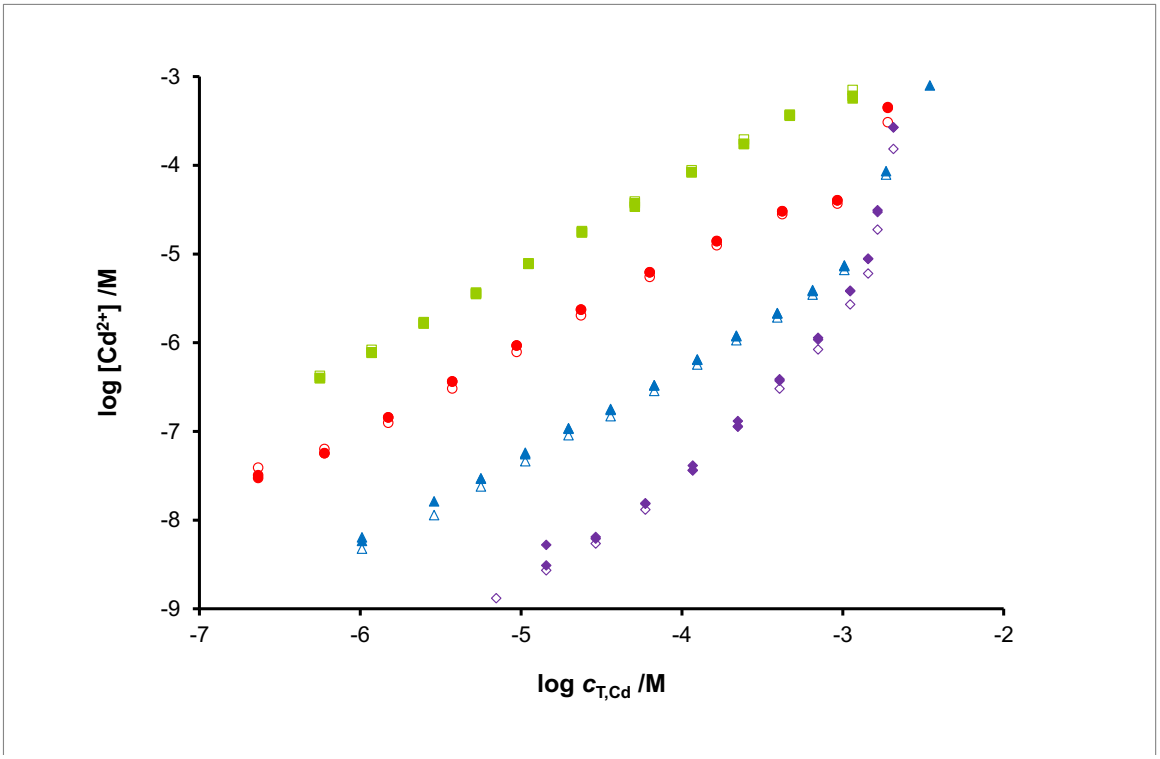

Figure 2: Free Cd concentration measured with AGNES-I (full markers) and with Cd-ISE (empty markers) at different pH (□for pH = 4; ○ for pH = 5; Δ for pH = 6 and ◊ for pH = 7). PAA concentration = 5×10^{-3} M and [KNO_3] = 0.1M. $Y_{1,a} = 10^{10}$, $t_{1,a}$ = 70 s, $Y_{1,b}$ = 100 s, $t_{1,b}$ = 210 s.

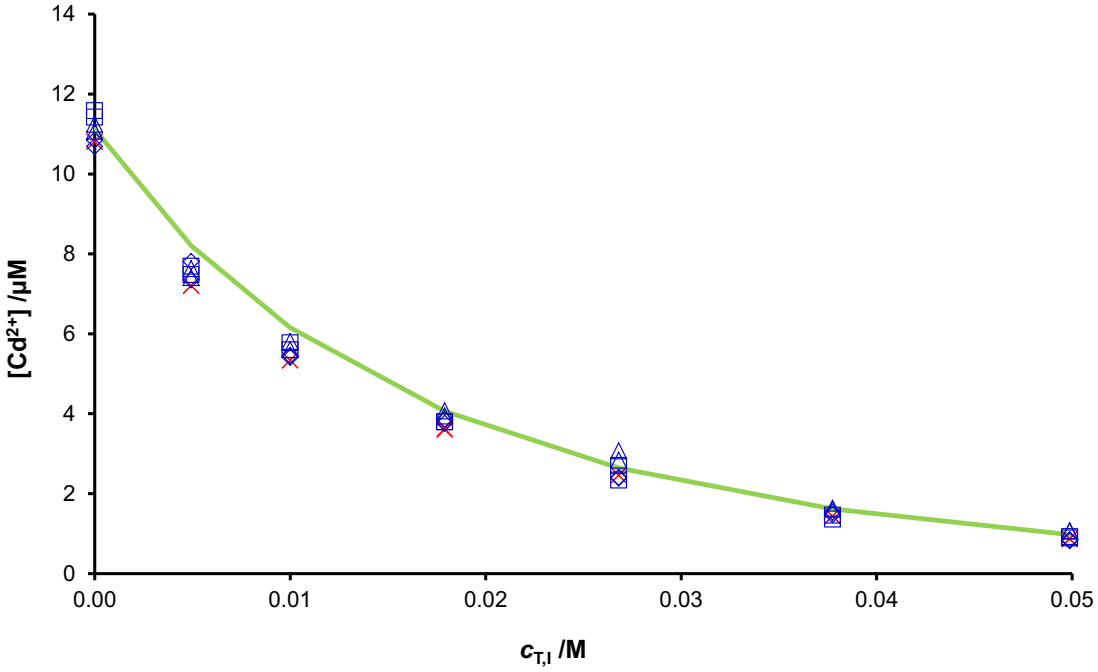

641

642 Figure3: Free Cd concentration for different total iodide concentrations ($c_{T,I}$) added to a
643 solution with initial total Cd concentration $c_{T,Cd}$= 1.24×10^{-5}M at pH= 6. Markers (×)
644 correspond to the data obtained from AGNES-I, (Δ) to AGNES-Q, (□) to AGNELSV, (◊)
645 to AGNES-SCP and green solid line to VMinteq prediction.

646

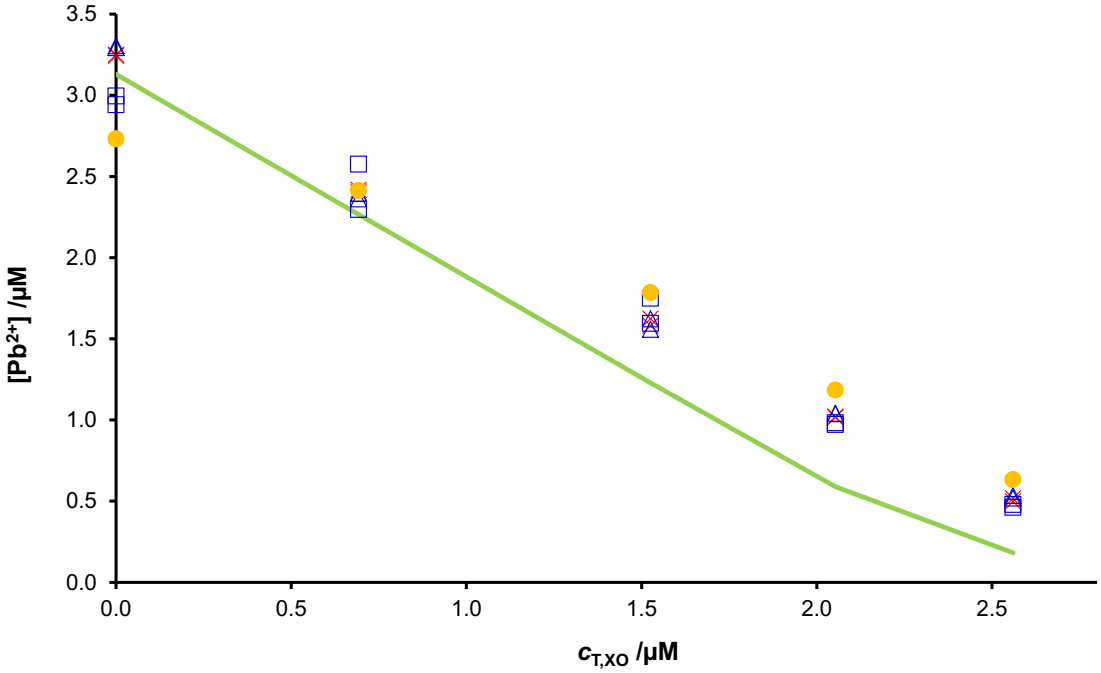

Figure 4: Plot of $[Pb^{2+}]$ vs $c_{T,XO}$ in a solution with initial $c_{T,Pb}$= 5.01x10^{-6} M and different XO concentrations. pH= 6.090 (buffer MES 0.01M). Markers: (×) correspond to the data obtained from AGNES-I, (Δ) to AGNES-Q, (□) to AGNELSV and (●) to ISE. The green line corresponds to a VMINTEQ calculation.

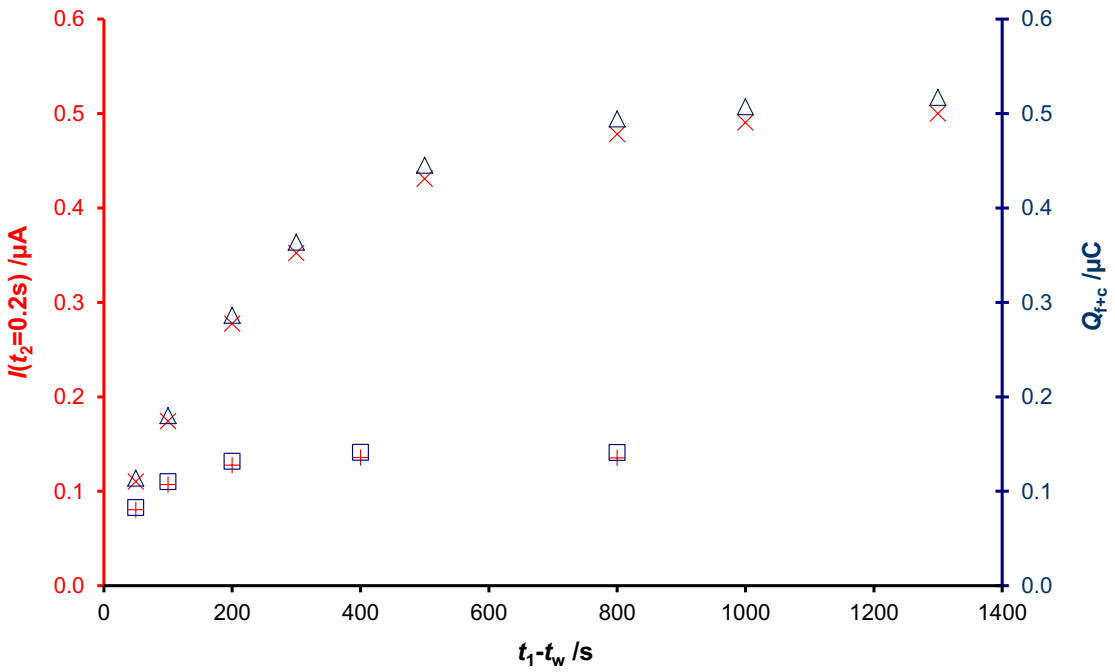

653

654 Figure 5: Trajectories of current (blue markers referred to the right ordinate axis) and
655 charge (red markers referred to the left ordinate axis) *vs.* deposition time (t_1-t_w with
656 t_w=50s) for two gains: *Y*=50 (+ and □) and *Y*=200 (× and Δ). $c_{T,Pb}$= 4.99x10^{-6}M, $c_{T,XO}$=
657 2.08x10^{-6}M and pH=6.104 (buffer MES 0.01M)

658

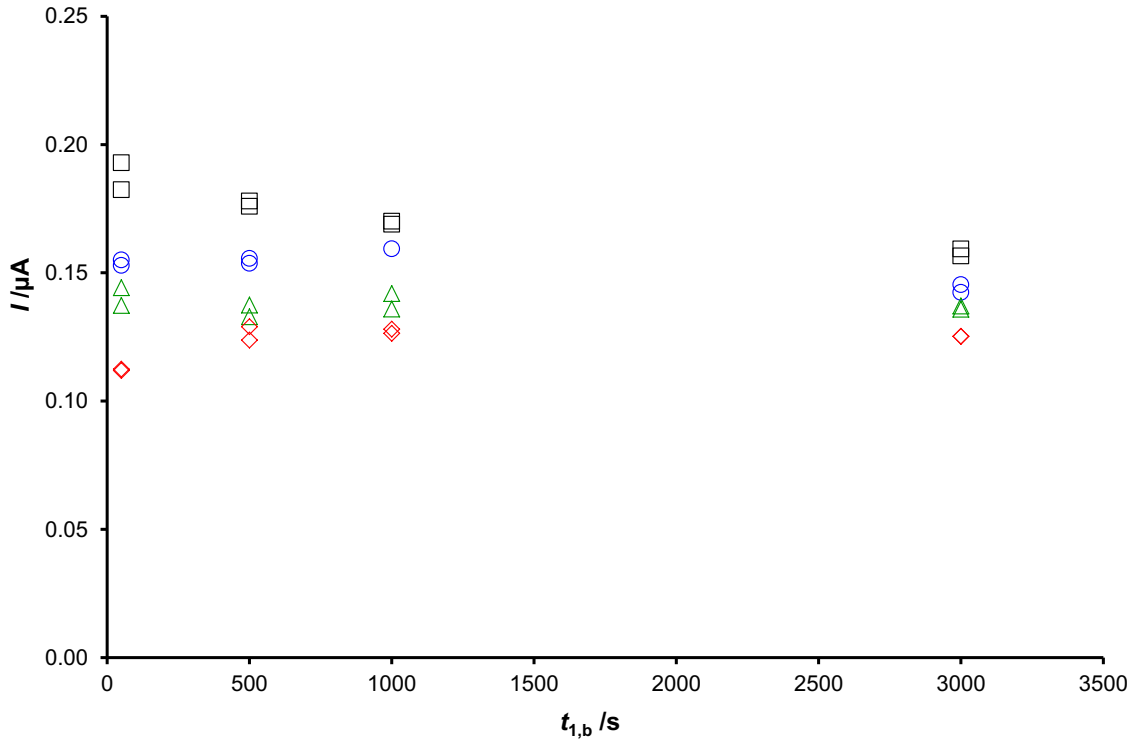

659

660 Figure 6 Currents leading to an unresolved free metal concentration with the standard
661 application of AGNES (stirring along $t_{1,a}$ and $t_{1,b}$; no stirring along t_w=50s) to a Nanotek
662 ZnO dispersion. Parameters: $Y_{1,a}=10^{12}$; $Y=Y_{1,b}=10$; $Y_2=10^{-10}$; t_2=50 s. Markers: (◊) for
663 $t_{1,a}$=3s; (Δ) for $t_{1,a}$=4s; (○) for $t_{1,a}$=5s and (□) for $t_{1,a}$=6s.
664

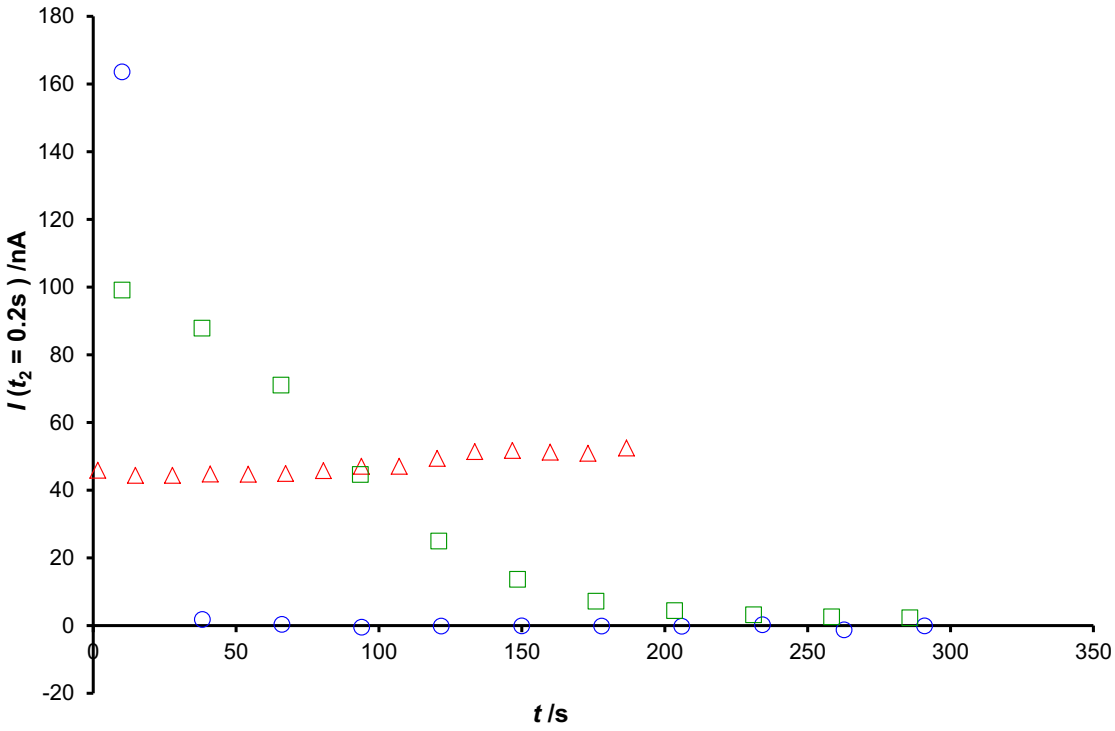

Figure 7: Plot showing that stirring favours the quick dispersant blockage of the electrode for the Zn^{o}/Zn^{2+} process, while extreme gains break it. A unique drop is used for each series along which a common procedure (where equilibrium is not reached) is repeated. Series with markers (○): Y_1=10, t_1=10s (with stirring), t_w=0. Series with (□): Y_1=10 ,t_1=t_w=10s (no stirring during deposition stage). Series with (Δ): Y_1=10^{12}, t_1=t_w=1.5s (no stirring). Currents are measured at t_2=0.2 s of the stripping stage which lasts 5 s and are represented *vs.* the time since the birth of the drop. In all experiments Y_2=10^{-10}. The medium contained a dispersion of Nanotek ZnO NPs approximately 2×10^{-4}M at pH=8.25.

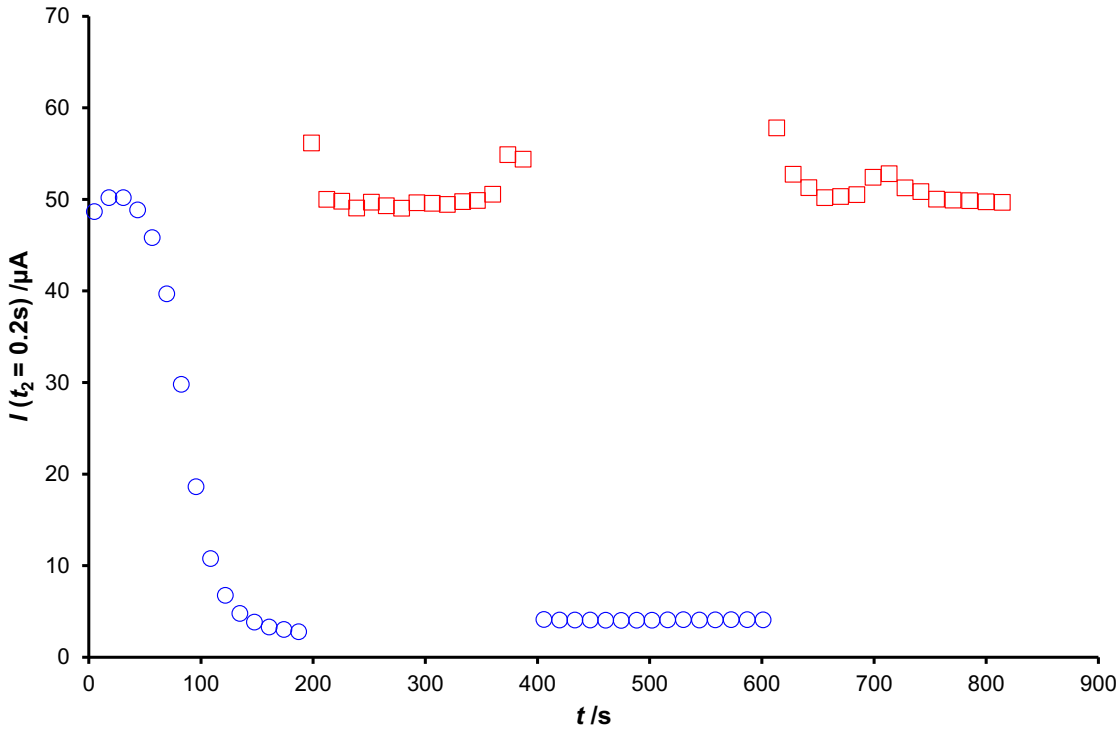

675

676 Figure 8: Ancillary experiments of current *vs.* drop lifetime showing that the surfactant is
677 not removed from the electrode surface after the application of a very negative potential.
678 Only one drop was used for all the data in this plot. Red square markers (□) represent
679 subseries with parameters $Y_1=10^{12}$, $t_1=t_w=1.5$s (no stirring during deposition stage) with
680 total stripping time $t_2=8.5$s. Blue circle markers (○) stand for subseries where $Y_1=10$,
681 $t_1=t_w=5$s (no stirring) and $t_2=5$s. In all cases $Y_2=10^{-10}$.

682

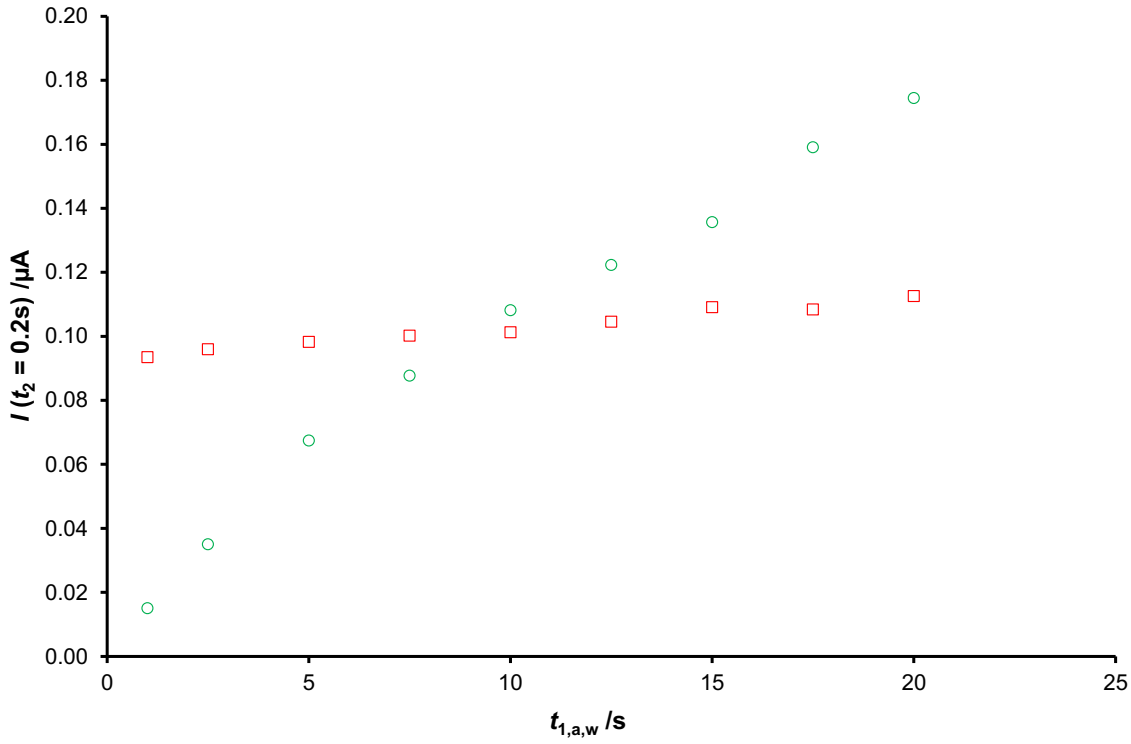

683

684 Figure 9: Finding of an optimized $t_{1,a,w}$ for Y=5 at the intersection of both series of
685 ancillary experiments. No stirring in any substage. Green circles (○) stand for
686 experiments of type Exp1 with $Y_1=10^{12}$. Red squares (□) stand for experiments of type
687 Exp2 with $Y_{1,a}=10^{12}$, $Y_{1,b}=5$ and $t_{1,b}=0$;$t_w=100$s. A different drop per marker and
688 experiment. In all cases $Y_2=10^{-10}$. The medium contained a dispersion of Nanotek ZnO
689 NPs approximately 2×10^{-4}M at pH=8.29.

690

691

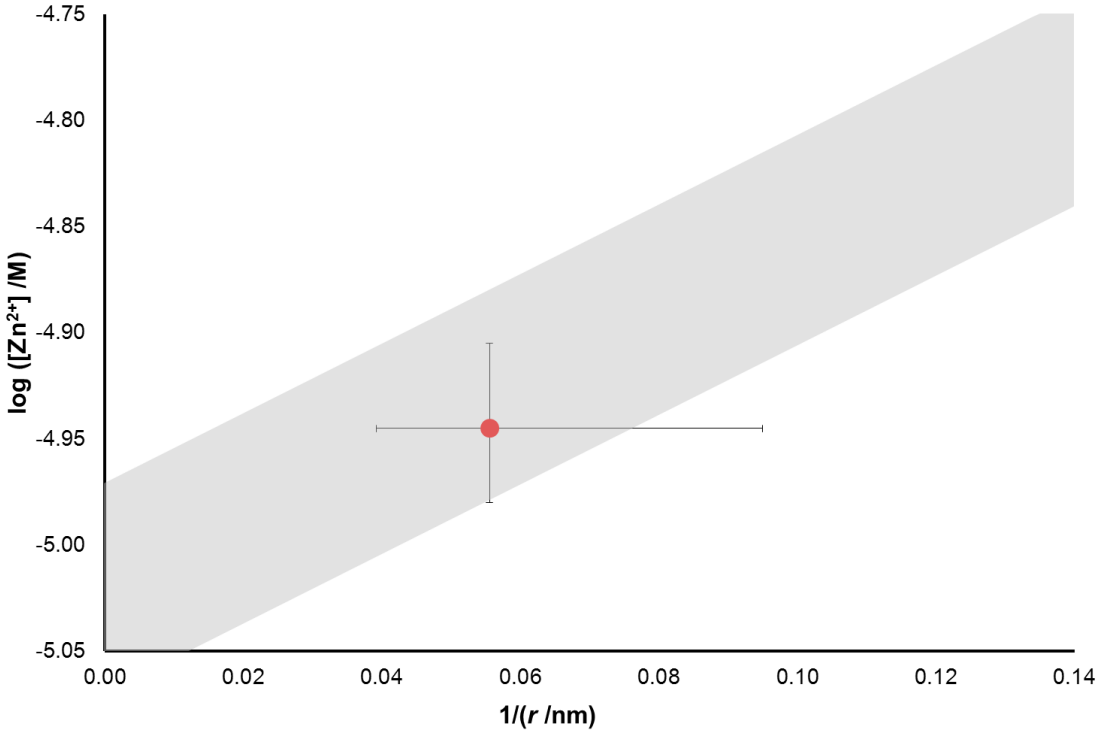

692

693 Figure 10: Diagram of the logarithm of equilibrium free Zn concentration *vs.* the inverse
694 of the radius of the ZnO nanoparticles. The red bullet indicates the average experimental
695 concentration retrieved by AGNES (average of Table 1 and other experiments) in a
696 dispersion of NanotekZnO NPs. The vertical error bar corresponds to the error in
697 AGNES determinations. The horizontal error bar indicates the estimated range of the
698 nanoparticle diameters 36±15 nm. The shaded region stands for the theoretical values
699 according to eqns. 3 and 5 in ref [26] taking into account the pH uncertainty 8.2 ±0.1.

700

701

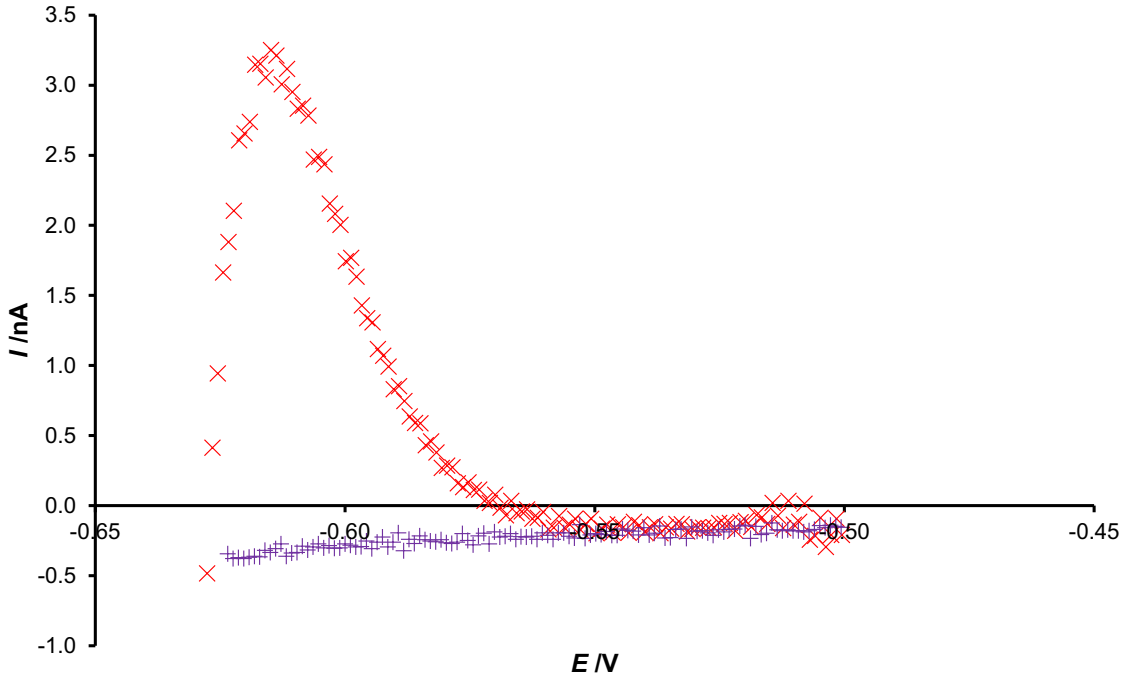

702

703 Figure 11: Evolution of the stripping current along the potential scan of an AGNELSV
704 experiment where scan rate = 0.008 V/s. $c_{T,Cd}$= 1.15x10^{-5}M, $c_{T,I}$= 9.53x10^{-2}M (×) and pH=
705 6.020. The (+) signs correspond to the synthetic blank (just the background electrolyte
706 0.1M KNO_3).